



**HAL**  
open science

# Impact of particle field heterogeneity on the dynamics of turbulent two-way coupled particulate flows

Roxane Letournel, Frédérique Laurent, Marc Massot, A. Vié

## ► To cite this version:

Roxane Letournel, Frédérique Laurent, Marc Massot, A. Vié. Impact of particle field heterogeneity on the dynamics of turbulent two-way coupled particulate flows. 10th International Conference on Multiphase Flow, ICMF 2019, May 2019, Rio de Janeiro, Brazil. hal-02392723

**HAL Id: hal-02392723**

**<https://hal.science/hal-02392723>**

Submitted on 4 Jun 2020

**HAL** is a multi-disciplinary open access archive for the deposit and dissemination of scientific research documents, whether they are published or not. The documents may come from teaching and research institutions in France or abroad, or from public or private research centers.

L'archive ouverte pluridisciplinaire **HAL**, est destinée au dépôt et à la diffusion de documents scientifiques de niveau recherche, publiés ou non, émanant des établissements d'enseignement et de recherche français ou étrangers, des laboratoires publics ou privés.

# Impact of particle field heterogeneity on the dynamics of turbulent two-way coupled particulate flows

Roxane Letournel<sup>1,2,3</sup>, Frédérique Laurent<sup>1,2</sup>, Marc Massot<sup>3</sup>, and Aymeric Vié<sup>1,2</sup>

1. Laboratoire EM2C, CNRS, CentraleSupélec, Université Paris-Saclay, 3 rue Joliot Curie, 91192 Gif-sur-Yvette cedex, France

2. Fédération de Mathématiques de CentraleSupélec, CNRS FR-3487, CentraleSupélec, Université Paris-Saclay,  
9 rue Joliot Curie, 91190 Gif-sur-Yvette cedex, France

3. CMAP, École Polytechnique Route de Saclay, 91128 Palaiseau cedex, France

roxane.letournel@centralesupelec.fr

**Keywords:** Particle dynamics, homogeneous isotropic turbulence, two-way coupling, heterogeneity

## Abstract

A series of coupled direct numerical simulations of decaying Homogeneous Isotropic Turbulence are performed on a  $128^3$  periodic box, with a size monodisperse population of particles at different Stokes numbers  $St$ , mass loading  $\phi$  and particle number densities  $n_0$  (mean number of particles per unit volume). Indeed, mechanisms for turbulence enhancement or suppression depend on these three combined parameters. Like previous investigators, crossover and modulations of the fluid energy spectra were observed consistently with the change in Stokes number and mass loading. Additionally, we also investigate the impact of the particle number density, which was not properly and independently characterized. This parameter plays a key role in the statistical convergence of the disperse phase and is therefore of primary importance for modeling purposes. DNS results show a clear impact of this parameter, promoting the energy at small scales while reducing the energy at large scales. Our investigation focuses on the identification of the energy transfer mechanisms, to highlight the differences between the influence of a homogeneous disperse phase (very high particle number density where statistical convergence is obtained) and heterogeneous cases (low particle number density). In particular, different regimes have been identified and described in terms of particle number density.

## Introduction

In the literature, the interactions between a turbulent carrier phase and a particulate phase in the point-particle limit have been extensively studied. In the one-way coupled context, for which the particles do not affect the carrier phase, the importance of Stokes number based on Kolmogorov or Lagrangian Integral time scales have been evidenced: the former characterises the occurrence of preferential concentration (Eaton and Fessler 1994) while the latter is representative of the transition to particle-trajectory-crossing dominated flows (Février et al. 2005).

In two-way coupled flows, focus has been made on the modulation of the turbulence spectrum depending on the Stokes number or the mass loading of particles. Squires and Eaton (1990); Boivin et al. (1998); Mallouppas et al. (2017) used a stationary HIT and showed that the turbulent kinetic energy was reduced by particles and that the reduction was weakly dependant on the Stokes number. However, Elghobashi and Truesdell (1993); Ferrante and Elghobashi (2003); Abdelsamie and Lee (2012) worked with a decaying HIT and found that particles with low Stokes number can enhance the fluid energy. Indeed, studies on the fluid-particle interaction spectrum reveals a negative contribution at low wave numbers that is reducing when

Stokes number increases, whereas the energy rate at large wavelengths remains positive. Druzhinin and Elghobashi (1999); Druzhinin (2001) focused on microparticles and provided an analytic expression of the coupling term in the limit of very small Stokes number. Ferrante and Elghobashi (2003) classified particles according to their Stokes number and described the evolution of turbulent energy and dissipation of the flow. Influence of mass loading was also investigated in some of the previous works, as well as in Squires and Eaton (1994) who described the effect of mass loading on turbulence dissipation rate. Consistently with previous studies, Sundaram and Collins (1999) concluded in their work that the shift in energy to high wavenumbers in the fluid phase increases the viscous dissipation rate.

The interest in the influence of the Stokes number and mass loading is easily justified by the fact that the former parameter globally determines the dynamics of particles in a given fluid and the latter plays a role in the inverse-coupling force that the particles exert on the fluid. However, a third parameter is necessary to fully characterize the disperse phase and thus its impact on the gaseous phase: the particle number density, which was never directly investigated to the author's knowledge. In fact, this parameter plays a key-role: for high number density, the proximity of particles can

lead to a continuous phase behavior, while for low number density, distant particles can produce local effects and the exact location of the particles may have a great impact on the dynamics of the flow. In the literature, it has been shown that, either in one-way or two-way coupled case, the particulate phase can reach a statistical convergence for a high initial number density, while for low initial number density, different dynamics can be observed (Vié et al. 2016). This statistical characteristic of the disperse phase is here referred as particulate phase heterogeneity. This effect must not be mistaken for preferential concentration, which results from the interaction of the disperse phase with turbulence and not for a potential lack in overall statistical convergence.

In the present work, we propose to investigate the effect of this parameter along with the mass loading and the Stokes number, to clearly identify the impact of the particulate phase heterogeneity on turbulence. We first present the assumptions and governing equations of our study (section 1). A decaying HIT loaded with particles is used here with DNS resolution of the flow and particle-point approach (section 1.5). Turbulence modulation by particles is then measured through the analysis of global energy transfers (section 2.1). A deeper insight is given by an analysis in the spectral domain (section 2.2), permitting to identify specific regimes with respect to the number density of the particulate phase.

## 1 Governing equations

### 1.1 Fluid and particles equation

We consider monodisperse solid spherical particles of fixed size. Particles diameter is smaller than the Kolmogorov length scale ( $d_p \ll \eta$ ), thus particle-resolved DNS is not necessary (Fröhlich et al. 2018), and a point-particle approximation is adopted. The density ratio between the particles and the fluid is large ( $\rho_p \gg \rho_f$ ) and the Reynolds number of the particle is smaller than one ( $Re_p \leq 1$ ). The volume fraction  $\alpha$  is small enough to consider particle-particle collisions as negligible (dilute regime:  $\alpha < 10^{-4}$ ). Therefore, many of the forces in the original Basset-Boussinesq-Oseen equation are assumed negligible compared to the drag force. Furthermore, if the drag force obeys Stokes' law, the equation of motion is linear in the velocity difference between fluid and particle. Then the motion equations of particles are written as

$$\begin{cases} \frac{d\mathbf{x}_p(t)}{dt} = \mathbf{v}_p(t) \\ \frac{d\mathbf{v}_p(t)}{dt} = \frac{\mathbf{u}_{f@p}(t) - \mathbf{v}_p(t)}{\tau_p} \end{cases} \quad (1)$$

where  $\mathbf{x}_p(t)$  and  $\mathbf{v}_p(t)$  stand for particle position and velocity at time  $t$ , and  $\mathbf{u}_{f@p}(t) = \mathbf{u}_f(t, \mathbf{x}_p(t))$  is the fluid velocity evaluated at the particle position. The particle relaxation time  $\tau_p$  is defined as  $\tau_p = \frac{\rho_p d_p^2}{18\mu_f}$  where  $\mu_f$  is the dynamic viscosity of the fluid. The effects of particles on the carrier phase are expressed through an additional force in the momentum equation of the fluid. For an incompressible fluid, the equa-

tions of motion for the carrier fluid are:

$$\begin{cases} \frac{\partial u_{f,i}}{\partial x_i} = 0 \\ \frac{\partial u_{f,i}}{\partial t} + \frac{\partial u_{f,i} u_{f,j}}{\partial x_j} = \frac{-1}{\rho_f} \frac{\partial P}{\partial x_i} + \frac{\mu_f}{\rho_f} \frac{\partial^2 u_{f,i}}{\partial x_i \partial x_j} + \frac{1}{\rho_f} f_i \end{cases} \quad (2)$$

where  $\mathbf{f}$  is the force exerted by particles on the fluid.

### 1.2 Coupling of equations

A projection kernel  $\Delta$  is introduced to give a local spatial average of the feedback force:

$$\mathbf{f}(\mathbf{x}, t) = \sum_p \mathbf{F}^{(p)} \Delta(\mathbf{x} - \mathbf{x}_p(t)) \quad (3)$$

where  $\mathbf{F}^{(p)} = m_p \frac{\mathbf{u}_{f@p}(t) - \mathbf{v}_p(t)}{\tau_p}$  is the resultant force exerted by a particle  $p$  of mass  $m_p$  on the fluid. In return, the local fluid velocity should be evaluated by applying the spatial filter at particle location:

$$\mathbf{u}_{f@p}(t) = \mathbf{u}_f(\mathbf{x}_p, t) = \int \Delta(\mathbf{x} - \mathbf{x}_p) \mathbf{u}_f(\mathbf{x}, t) d^3\mathbf{x} \quad (4)$$

The choice of the projection kernel depends on the developed physics or the desired precision. Thus, Strutt et al. (2011) discussed the accuracy of interpolation schemes such as the fourth-order cubic spline, the fifth-order Lagrange or the third-order Hermite polynomials interpolation. Maxey et al. (1997) also proposed a "narrow envelope function" in the form  $\Delta(\mathbf{x}) = (2\pi\sigma^2)^{-3/2} \exp(-\mathbf{x}^2/2\sigma^2)$ , that can be adjusted with parameter  $\sigma$ , which was used by other works (Capecelatro and Desjardins 2013; Zamansky et al. 2014).

Spatial averages can therefore be defined as:

$$n(\mathbf{x}, t) = \int \sum_p \Delta(\mathbf{x} - \mathbf{x}_p(t)) d^3\mathbf{x} \quad (5)$$

$$\tilde{\mathbf{v}}_p(\mathbf{x}, t) = \frac{1}{n(\mathbf{x}, t)} \int \sum_p \mathbf{v}_p \Delta(\mathbf{x} - \mathbf{x}_p(t)) d^3\mathbf{x} \quad (6)$$

$$\tilde{\mathbf{u}}_{f@p}(\mathbf{x}, t) = \frac{1}{n(\mathbf{x}, t)} \int \sum_p \mathbf{u}_{f@p} \Delta(\mathbf{x} - \mathbf{x}_p(t)) d^3\mathbf{x} \quad (7)$$

For monodisperse spherical particles,  $m_p = \rho_p \pi d_p^3/6$  and global volume fraction is defined as  $\alpha = n_0 \pi d_p^3/6$ , where  $n_0$  is the mean particle number density  $\langle n(\mathbf{x}, t) \rangle = n_0$ . The mass loading of the disperse phase is therefore defined as  $\phi = \alpha \rho_p / \rho_f$ . In the following, we focus on the study of the fluid-particle interaction term defined by:

$$\frac{1}{\rho_f} \mathbf{f}(\mathbf{x}, t) = \phi \frac{n(\mathbf{x}, t)}{n_0} \frac{\tilde{\mathbf{v}}_p(\mathbf{x}, t) - \tilde{\mathbf{u}}_{f@p}(\mathbf{x}, t)}{\tau_p} \quad (8)$$

### 1.3 Kinetic energy equation

To evaluate turbulence modulation by particles, statistical quantities and spectrum of energy are studied. The time-evolution equation of turbulent kinetic energy  $e(t)$  is obtained by multiplying fluid momentum equation by  $u_{f,j}$  and ensemble averaging:

$$\frac{de(t)}{dt} = -\epsilon(t) + \psi_p(t) \quad (9)$$

where  $\epsilon(t) = 2\nu\langle S_{ij}S_{ij} \rangle$  is the viscous dissipation rate of  $e(t)$  with  $S_{ij} = \frac{1}{2}(\frac{\partial u_{f,i}}{\partial x_j} + \frac{\partial u_{f,j}}{\partial x_i})$  and  $\nu_f$  is the dimensionless kinematic viscosity.  $\psi_p(t)$  represents the energy rate of change due to the particles drag force:

$$\psi_p(t) = \frac{\phi}{\tau_p n_0} \left\langle n(\mathbf{x}, t) u_{f,i}(\mathbf{x}, t) [\tilde{v}_{p,i}(\mathbf{x}, t) - \tilde{u}_{f@p,i}(\mathbf{x}, t)] \right\rangle \quad (10)$$

Performing the Fourier transform of the fluid momentum equation, we obtain the equation for the energy spectrum  $E(\kappa)$ :

$$\frac{dE(\kappa, t)}{dt} = T(\kappa, t) - D(\kappa, t) + \Psi_p(\kappa, t) \quad (11)$$

where the spectral dissipation rate is  $D(\kappa) = 2\nu_f \kappa^2 E(\kappa)$  and  $T(\kappa)$  is the spectral energy transfer rate. The fluid-particle energy interaction term  $\Psi_p(\kappa)$  produced by particles is responsible for the modulation in the turbulence energy spectrum.

#### 1.4 Interdependence of parameters

The difficulty in predicting particle-turbulence interactions is due to the number of physical quantities involved. In principle, the system is described by the dispersed phase characteristics (mass, volume of a particle, number of particles...) and the turbulence characteristics (length, time and velocity scales). However, these primary parameters are not necessarily the most relevant to understand the results of a simulation. There are many "derived" quantities such as particle response time  $\tau_p$ , or particle number density  $n_0$ .

Thus, as presented in Fig. 1a, we have selected three common parameters necessary to describe the particles: the density of their material  $\rho_p$ , their size, here related to the diameter  $d_p$  and the number of particles in the domain, described through the mean particle number density  $n_0$ . Other parameters can be deduced from those three and are related to each other in blue in Fig. 1a: the mass of particles  $m_p$  and the volume fraction  $\alpha$ .

Regarding some properties of the turbulence flow, dimensionless numbers can be derived, considering fluid density  $\rho_f$ , Kolmogorov time  $\tau_k = (\nu_f/\epsilon)^{1/2}$  and length scale  $\eta = (\nu_f^3/\epsilon)^{1/4}$ . This yields the ratio of the characteristic time of a particle and a turbulence time scale, commonly referred to as the Stokes number  $St = \tau_p/\tau_k$ , the ratio of the diameter of particles and Kolmogorov length scale  $d_p/\eta$  and the dimensionless particle number density, introduced by Poelma et al. (2007), noted  $n_\eta = n_0\eta^3$ , that can be interpreted as the number of particles per Kolmogorov eddy. All those parameters are related to each other in Fig. 1b.

Given a fluid and turbulence properties, only three fundamental units are present: time, mass and length. According to the  $\Pi$ -theorem, the system is describable by only three dimensionless parameters of diagram 1b, each of which must belong to a different "group" (symbolized with the circles in the background of Fig. 1).

The reader can re-examine previous publications under the scope of this diagram. Table 1 shows the choices of

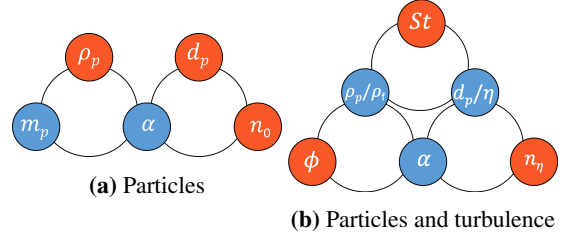


**Figure 1:** Interdependence of dispersed phase parameters for particles only (a) and for particles in turbulence (b).

parameters fixed and studied (in bold font in the "changed" column) in previous studies. The only consistent and exhaustive study of a given triplet was completed by Elghobashi and Truesdell (1993) who successively observed the separate influence of  $\tau_p$ ,  $\alpha$  and  $d_p$ . However, the extensive use of computational particles to represent one real particle ( $M_r/M_c = 100$ ) can show the bias of an heterogeneous disperse phase. As already noticed in Boivin et al. (1998), neither simulations of Squires and Eaton (1990); Elghobashi and Truesdell (1993) nor their own calculations met the condition of  $n_\eta \gg 1$ , required for correspondence between computational and actual particles. Therefore, only "real" particles ( $M_r/M_c = 1$ ) are used in our study.

Our choice of description for the disperse phase is represented by the orange triplet in Fig. 1b. The choice of these three parameters was made in view of the proposed form of the interaction term. Indeed, in Eq. 10, mass loading is a factor as well as the inverse of the relaxation time of the particles. We therefore naturally wanted to be able to study the influence of each of these terms in modifying turbulence.

For the description of the system, we see in Fig. 1b that the third parameter can be the volume fraction, the particle diameter or the particle number density. From a modeling point of view, we have already seen that the number of particles plays a role in the description of the disperse phase in single-phase flows (Vié et al. 2016). We will see through this work that at fixed Stokes and mass loading, particle distribution in space is essential to quantify the impact on the gaseous phase.

In some of previous works such as those of Druzhinin and Elghobashi (1999); Druzhinin (2001), particle field has been considered as perfectly homogeneous when  $St \ll 1$ . This assumption was justified by considering that in the case of microparticles the preferential accumulation is negligible. However, if particle number density is not large enough, the disperse phase cannot be considered as homogeneous even though the distribution of particles is uniform in the domain. One of the aim of this present work is to give a criterion on particle number density to determine if the disperse field is homogeneous and therefore the inverse effect on the fluid has as well an homogeneous limit.

#### 1.5 Numerical Framework

The proposed test case is a decaying homogeneous isotropic turbulence loaded with particles. The domain is a cubic periodic box of size  $L = 5$ . The initial condition for the gaseous phase is set using a Pope spectrum (Pope 2000). The prescribed initial microscale Reynolds number is  $Re_\lambda = 18$  with  $\nu_f = 0.001$  and  $u_{rms}(t = 0) = 0.1$ . Initial

Reference	Forcing	$M_r/M_c$	Fixed	Changed
Squires and Eaton (1990)	YES	100	$\tau_p, n_\eta$	$\phi, \alpha, \rho_p, d_p$
Elghobashi and Truesdell (1993)	NO	100	$\alpha, \tau_p$	$d_p, \phi, n_\eta, \rho_p$
			$\alpha, d_p, n_\eta$ $\tau_p, \rho_p, d_p$	$\tau_p, \rho_p, \phi$ $\alpha, \phi, n_\eta$
Squires and Eaton (1994)	YES	1	$\tau_p, n_\eta$	$\phi, \alpha, \rho_p, d_p$
Boivin et al. (1998)	YES	> 1	$\alpha, \phi, \rho_p$	$\tau_p, d_p, n_\eta$
			$\tau_p, n_\eta$	$\phi, \rho_p, \alpha, d_p$
Druzhinin and Elghobashi (1999)	NO	1	$\tau_p, \rho_p, d_p$	$\phi, \alpha, n_\eta$
Sundaram and Collins (1999)	NO	1	$\alpha, \phi, \rho_p$	$\tau_p, d_p, n_\eta$
			$\tau_p, d_p, \rho_p$	$\alpha, \phi, n_\eta$
Druzhinin (2001)	NO	1	$\alpha, \phi, \rho_p$	$\tau_p, d_p, n_\eta$
Ferrante and Elghobashi (2003)	NO	47	$\alpha, \phi, \rho_p$	$\tau_p, d_p, n_\eta$
Abdelsamie and Lee (2012)	YES vs NO	95	$\alpha, \phi, \rho_p$	$\tau_p, d_p, n_\eta$
Mallouppas et al. (2017)	YES	1	$\alpha, d_p, n_\eta$	$\tau_p, \rho_p, \phi$
			$\tau_p, \rho_p, d_p$	$\phi, \alpha, n_\eta$

**Table 1:** Previous studies of the modulation of turbulence by disperse phase. Forcing scheme for stationary HIT and ratio of real particles per computational particle are precised for each study. Choice of fixed parameters and studied parameters are displayed in the two last columns.

integral length scale is  $\ell_0 = 0.22$  and Kolmogorov length scale  $\eta_0 = 0.02$ .

The particles are injected after approximately one eddy turnover time to ensure that natural turbulence has established itself. At injection time, the particle locations are randomly drawn in the domain, and the particle velocities are set equal to the ones of gas phase at the particle locations. The simulation is run under one-way coupling during approximately one eddy turn over time to “thermalise” the particles. Then the two-way coupled is activated and the evolution of the turbulence spectrum is analysed. This delay for the activation of the two-way coupling allows the influence of the particles to be studied once they have naturally segregated into a perfectly undisturbed homogeneous turbulence. This removes an inconvenient transitional regime observed otherwise, already mentioned in Ferrante and Elghobashi (2003), especially visible for particles with large Stokes.

We performed direct numerical simulation to solve the unsteady three-dimensional Navier-Stokes and continuity equations with the Asphodel code using a low Mach formulation of the Navier-Stokes equations and a Lagrangian formulation for the particles (Reveillon and Demoulin 2007). The time resolution is provided by a third order explicit Runge Kutta scheme and spatial evolution is done with a finite difference scheme.

As mentioned above, we are operating in such circumstances that the point-particle approach is suitable. In Fröhlich et al. (2018), the accuracy of such models with two-way coupling for particles of Kolmogorov-length-scale was assessed. A third-order interpolation algorithm is

used in order to compute the gaseous quantities at droplet location. To project the Lagrangian quantities of droplets onto the Eulerian gaseous grid nodes, the PSI-Cell method of Crowe et al. (1977) is used. The Lagrangian contributions are instantaneously allocated to neighboring gas nodes, weighted by the distance to the nodes. This method is sometimes controversial because it depends on refinement. However, as part of the work carried out here, we were able to verify with finer mesh grids ( $256^3$ ) that the refinement does not qualitatively nor quantitatively modify the impact of the same disperse phase on the studied energy spectra.

Another concern was the choice of forced or decaying HIT. Among the works mentioned above, we can distinguish studies with forced stationary turbulence, for which statistics are therefore easier to carry out, from naturally decreasing turbulences, as reported in Table 1. A comparison of these turbulences is proposed by Abdelsamie and Lee (2012), who noted a number of contradictions in the attempt to study the impact of particles on the energy spectrum even though it is artificially forced. Many differences are observed, including significant changes in the influence of small particles that do not allow energy to be reintroduced to the fluid in forced turbulence. And although Mallouppas et al. (2013) introduced a new forcing model, the same biases observed for small particles are found in their results. We have therefore chosen to place ourselves in decaying turbulence, but we choose to normalize the observed quantities by the total kinetic energy at each instant and thus retrieve more stationary trends in the evolution of components of the energy decay rate.

## 2 Results

In the present work, we apply direct numerical simulations to investigate turbulence modulation by inertial particles in decaying isotropic turbulence. Parameters of the disperse phase were successively varied to provide data on modulation of turbulence features and energy spectra. An overview of the evolution of statistical quantities is presented in 2.1, according to the three parameters  $St$ ,  $\phi$  and  $n_\eta$ . Then, details are given in section 2.2 with a spectral analysis of the fluid energy and the fluid-particle coupling energy rate. The results already observed in the literature for the influence of Stokes number and mass loading are retrieved, and the focus is on the role played by the particle number density, and the importance of taking it into consideration for a heterogeneous disperse phase. In section 2.2.3 we investigate the effect of a highly heterogeneous disperse phase composed of isolated particles and define this specific regime with a criterion on the particle number density.

### 2.1 Two-way interaction energy rate

The existing literature has agreed that there is a criterion for determining whether turbulence will be increased or decreased by the presence of particles. While some studies propose a diameter ratio on a turbulence scale, others have observed the importance of the role played by the Stokes number based on Kolmogorov time scale. Ferrante and Elghobashi (2003) suggest that the critical Stokes (based on

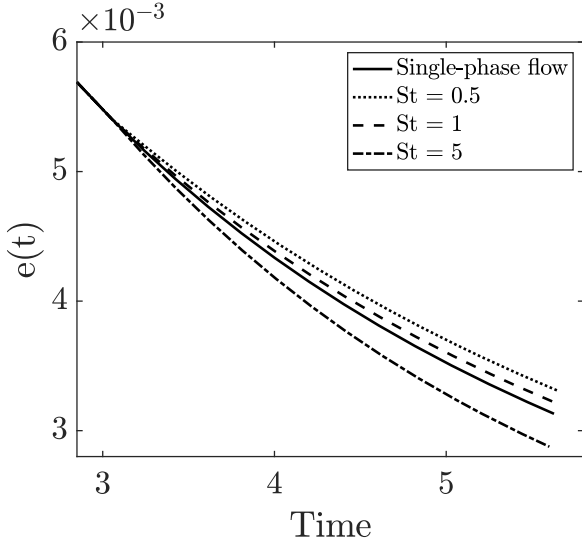
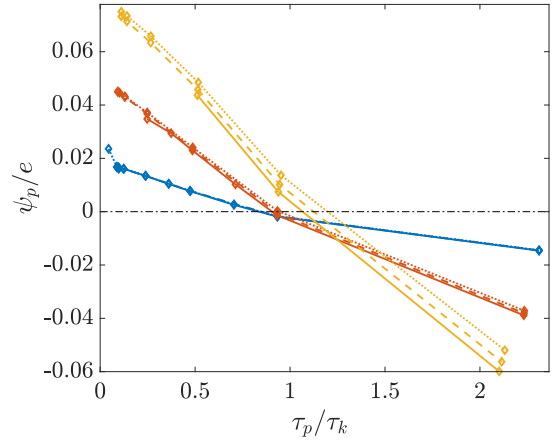


**Figure 2:** Turbulent kinetic energy and decay rate evolution for  $\phi = 0.3$  and a statistically converged disperse phase. Stokes are obtained with  $\tau_k(t = t_{inj})$

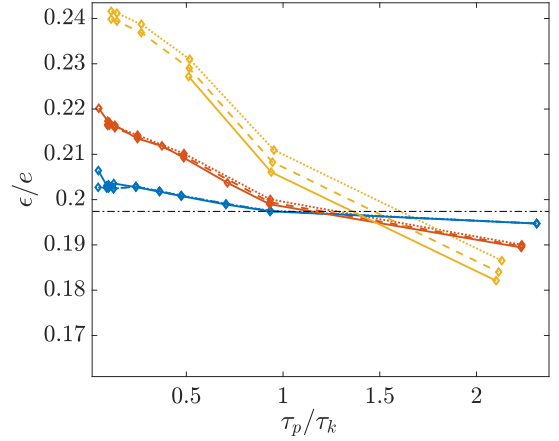
initial Kolmogorov time scale) is in the order of 0.25, and then name these particles as "ghosts" because of their limited influence on the total energy change of the turbulence. Figure 2 shows similar results: the Stokes number does play a role in the modulation of the kinetic energy of the fluid, with a tendency to slow down the rate of energy decrease for low Stokes, and to increase it for more inertial particles. The evolution equation of this decay rate is related to the dissipation term  $-\epsilon(t)$ , to which is added the energy rate of change due to particle drag force  $\psi_p(t)$ .

Figure 3 describes the evolution of the two components of the decay rate: the fluid-particle coupling energy rate (Fig. 3a) and the dissipation rate (Fig. 3b) at a given time  $t = 4.6$  and as a function of the Stokes number. The two energy rates have very similar behaviors, and the strain rate being only a function of the fluid, we deduce that fluid dissipation is closely related to the fluid-particle energy rate. This correspondence is clearly visible in Fig. 4 which groups the fluid dissipation values according to those of the fluid-particle exchange term. Moreover, the change in dissipation relative to the one for single-phase flow is smaller than the added term  $\psi_p$ . Therefore, we will mainly focus on the two-way interaction energy rate and consider the dissipation as a consequence of this term.

We measure a change in the sign of  $\psi_p$  around Stokes close to unity. Note that the Stokes calculated in our study is based on Kolmogorov scale at the measuring time, and not the injection time as it is defined in the article of Ferrante and Elghobashi (2003). In the case of  $St < 1$ , the fluid-particle coupling energy rate  $\psi_p$  is positive, because the fluid-particle correlation along the particles paths is larger than the auto-correlation of the fluid (Ferrante and Elghobashi 2003). In the scalar limit (for microparticles), the particle distribution is relatively uniform and particles behave like fluid-tracers. They are not ejected from the vortex cores and they retain their kinetic energy longer than the surrounding fluid. This is called "dusty gas", a phenomenon already described by



**(a)** Fluid-particle exchange energy rate



**(b)** Dissipation rate

**Figure 3:** Normalized fluid-particle exchange energy rate (a) and dissipation rate (b) versus Stokes number at time  $t = 4.6$ . Lines blue:  $\phi = 0.1$ , red:  $\phi = 0.3$ , yellow:  $\phi = 0.6$ , —:  $n_\eta = 2$ , ---:  $n_\eta = 0.2$ , .....:  $n_\eta = 0.1$ . The black dash-dotted line stands for the single-phase flow.

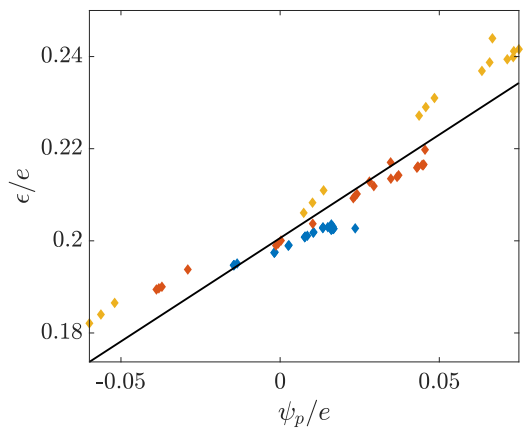


**Figure 4:** Normalized dissipation rate  $\epsilon/e$  as a function of  $\psi_p/e$ . at time  $t = 4.6$  For colors legend, refer to Fig. 3

Saffman (1962) and quantified analytically by the model of Druzhinin (2001). With the inverse coupling, particle energy is given to the fluid resulting in an attenuation of the energy decay rate. For Stokes numbers close to unity, particles are ejected from the large-vorticity cores but remain in their orbits. Even though fluid-particle energy rate is close to zero,

the accumulation of particles in those peripheric areas of vortices increases the dissipation.

Conversely, when the inertia of the particles increases, the fluid-particle coupling energy rate becomes negative due to a decorrelation between the velocities of the fluid and the particles. Inertial particles escape from their initial vortices and "cross" the trajectories of fluid points. Accordingly,  $\psi_p$  becomes negative and thus enhances the decay rate of turbulent kinetic energy.

As expected, an increase in mass loading produces a more significant fluid-particle coupling term. Figure 3a suggests that a normalization by a multiplicative coefficient close to  $\phi$  would yield a scaling independent of mass loading. Thus, at high Stokes, an increase in mass loading enhances the suppression of kinetic energy. On the contrary, at low Stokes,  $\psi_p$  remains positive, and its absolute value increases, which slows down the natural decrease in the turbulent kinetic energy of the fluid. Physically, the particles with low Stokes follow the fluid particles and thus uniformly charge the vortices, which therefore retain their vorticity longer.

Finally, Fig. 3a shows that the particle number density  $n_\eta$  influences the two-way interaction energy rate, especially when the mass loading  $\phi$  is large. Figure 5, which shows the evolution of the fluid-particle energy rate as a function of the particle number density, confirms that an heterogenous disperse phase enhances the fluid-particle exchange term contribution. In Fig. 3a, we also verify that the segregation (dotted lines) decreases as the number of particles increases. Segregation is defined as  $\langle n(\mathbf{x}, t)^2 \rangle / n_0^2$ . This convergence is solely a statistical effect (Law of Large Numbers) and is not related to a modification of the accumulation zones. This decrease was also observed and quantified by Vié et al. (2016). The asymptotic convergence of the disperse phase segregation with particle number density naturally leads to an asymptotic value for the fluid-particle exchange energy rate as well. However, the segregation does not appear to be modified by the mass loading of the particles (dashed lines of the three different values of  $\phi$  overlap in Fig. 5, indicating that the consideration of reverse coupling does not significantly change the segregation of the particles. Therefore, we can deduce that fluid-particle energy rate scales the segregation when normalized by a factor relative to the mass loading. This means that the higher the mass loading, the more important the particle number density is for the fluid-particle exchange term.

## 2.2 Spectral analysis

The consequence on the coupling can be further examined by taking the evolution of the energy spectra and the spectral coupling. Even for unchanged statistics, as it appears to be the case for Stokes number close to unity, energy spectra can be modified by particles.

In Fig. 6, the turbulence spectrum is plotted at time  $t = 4.6$  without particles, and in the two-way coupled cases for a mass-loading of 0.6, a droplet Stokes number of 2.2, and five different values of mean particle number densities:  $n_\eta = 0.02, 0.1, 0.2, 1, 2$ . It is shown that the presence of par-

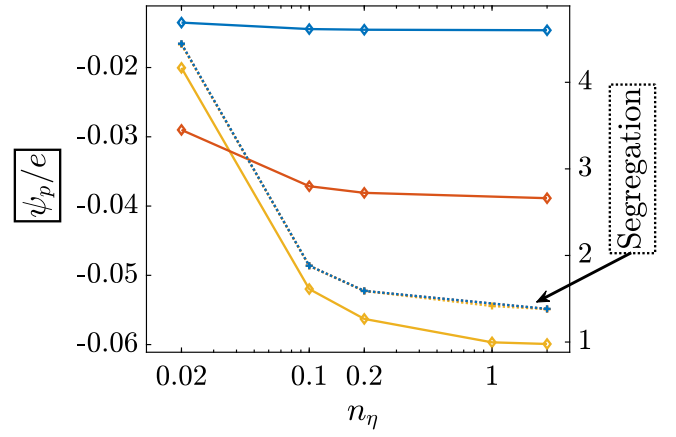


**Figure 5:** Fluid-particle coupling energy rate and segregation as a function of particle number density for  $St = 2.2$  at  $t = 4.6$ . Lines blue:  $\phi = 0.1$ , red:  $\phi = 0.3$ , yellow:  $\phi = 0.6$ , —: Fluid-particle coupling energy rate, .....: Segregation

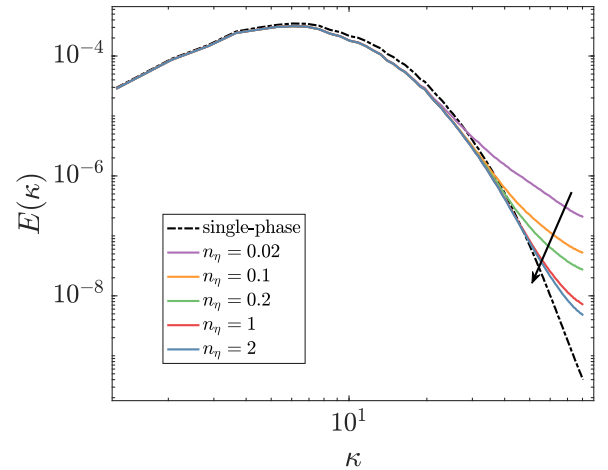
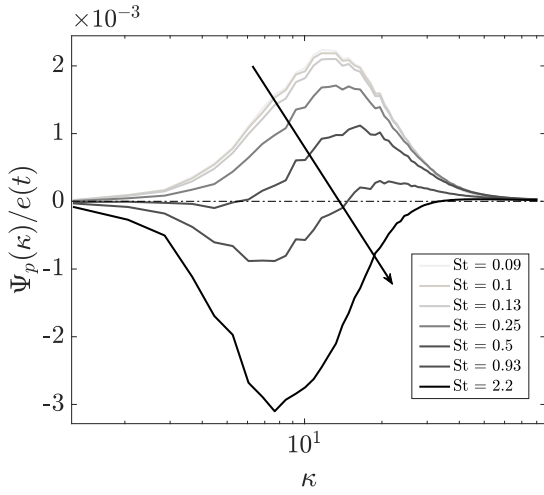


**Figure 6:** Energy spectrum at  $t = 4.6$  for  $\phi = 0.6$  and  $St = 2.2$ . The arrow shows the increase in the particle number density. The dash-dotted line stands for the single-phase flow spectrum.

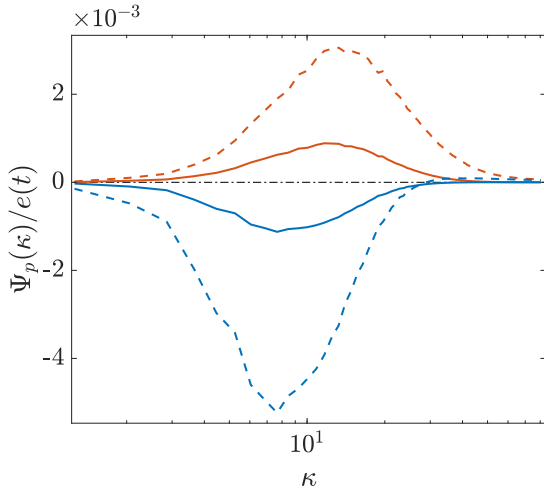
ticles enhances the energy at small scales while decreasing the energy at large scales, the overall turbulent kinetic energy being reduced because of the promoted turbulent dissipation. As the particle number density is increased, the spectrum tends to a homogeneous-limit one. In the next steps of this study, we will investigate the different regimes with respect to the droplet interspace  $\delta = 1/n_0^{1/3}$  compared to the Kolmogorov and the Integral length scales.

### 2.2.1 Influence of Stokes number and mass loading on the spectrum of fluid-particle energy modulation

The fluid-particle interaction spectrum has been extensively studied in the literature. In particular, Ferrante and Elghobashi (2003) compared  $\Psi_p(\kappa)$  for different Stokes number and found similar results. Figure 7a shows that for particles with small Stokes (microparticles),  $\Psi_p(\kappa)$  is positive at almost all wavelengths and thus produces a positive contribution to the decay rate  $\partial E(\kappa)/\partial t$ . On the other hand, the term is negative at almost all wavelengths for larger Stokes. For intermediate Stokes,  $\Psi_p(\kappa)$  remains positive for large  $\kappa$  while a negative peak appears in the spectrum for



(a) Influence of Stokes number (the arrow shows its increase) on  $\Psi_p$  spectrum. Fixed parameters are  $\phi = 0.3$  and  $n_\eta = 0.2$



(b) Influence of mass loading on  $\Psi_p$  spectrum. Lines red:  $St = 0.13$ , blue:  $St = 2.2$ , —:  $\phi = 0.1$ , - - -:  $\phi = 0.6$

**Figure 7:** Influence of Stokes number and mass loading on  $\Psi_p$  spectrum at  $t = 4.6$

small  $\kappa$ . It can be assumed that in the neighborhood of the particle, the fluid particles "follow" the inertial particle, thus producing a local correlation of particle velocity with the velocity of the surrounding fluid. This results in a positive interaction at high  $\kappa$  on the  $\Psi_p$  spectrum. Figure 7b shows the spectral fluid-particle interaction for two different Stokes and two different mass loading. As mentioned in section 2.1, the scaling between spectra with same Stokes but different mass loading could be the ratio of mass loading, but as measured in the total two-way interaction energy rate  $\psi_p(t)$ , it is not exactly the case due to the inverse coupling effect.

Figure 8 shows that the wavenumber  $\kappa_{cut}$  that characterizes the crossing on the spectrum (from negative to positive  $\Psi_p(\kappa)$ ) shifts to the right as the Stokes number increases. This reveals that the correlation of fluid velocity by particles is more and more localized and limited (to small scales) as particle inertia increases.

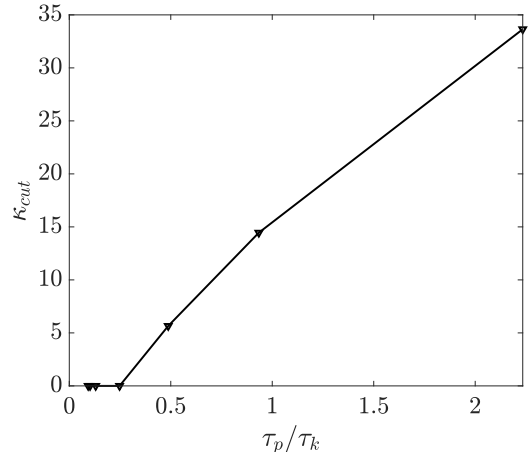


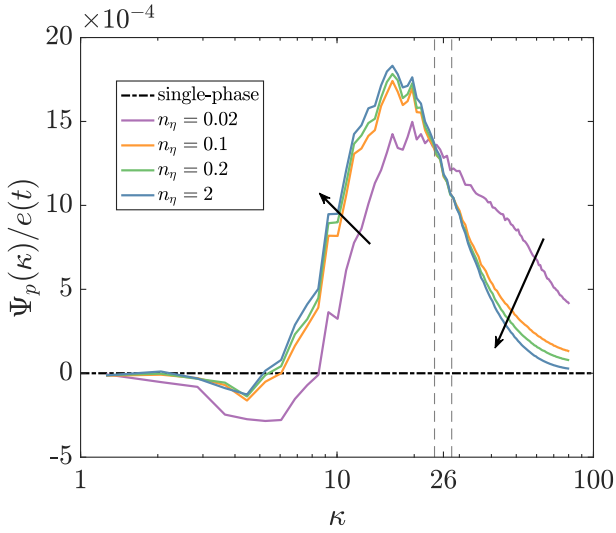
**Figure 8:**  $\kappa_{cut}$  as a function of Stokes number (fixed mass loading  $\phi = 0.3$ ). For  $St < 0.25$ , no crossing has been observed.

### 2.2.2 Influence of particle number density on the spectrum of fluid-particle energy modulation

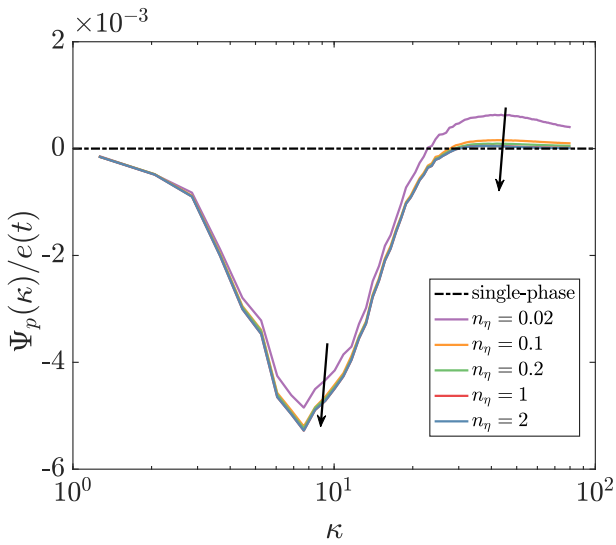
Results of section 2.1 show that a low particle number density results in an increase in the fluid-particle interaction energy rate  $\psi_p(t)$ , especially when the mass loading is high (Fig. 5). Let us study the spectrum of this exchange term to understand at what scales the interactions between particles and fluid are located and how the distribution of mass loading can modify the fluid energy. A high particle number density produces a homogeneous particle concentration field in which each particle is light and takes part in a collective cluster of particles. On the contrary, a low particle number density generates a heterogeneous particle concentration field and therefore individual particles are more isolated and heavy.

We can see in Figs. 9a and 9b that a heterogeneous disperse phase (purple line) produces a larger  $\Psi_p(\kappa)$  at small scales than a homogeneous one (blue line). However, for particles with small Stokes in Fig. 9a, this effect is reversed at large scales of the fluid and the homogeneous disperse phase produces a stronger source term. On the other hand, for particles with higher Stokes in Fig. 9b, the negative peak at large scales is enhanced by the collective effect of clustered particles. In both cases, at larger scales, the fluid-particle exchange of the heterogeneous disperse phase seems to be reduced (in absolute value) compared to the homogeneous one.

Figure 10 shows the spatial distribution of the local two-way interaction energy rate  $\tilde{\psi}_p(\mathbf{x}, t) = \mathbf{u}_f(\mathbf{x}, t)\mathbf{f}(\mathbf{x}, t)/\rho_f$ , with superimposed particles in a part of the flow domain at time  $t = 4.6$ . Particles parameters were set to the same Stokes number  $St = 0.25$ , and global mass loading  $\phi = 0.3$ , but different particle number densities. Figure 10a shows that each isolated particle produces a strong localized contribution to the two-way interaction term, and therefore the two-way interaction field is strongly heterogeneous, accordingly to the corresponding particle concentration field. By increasing the particle number density  $n_\eta$  without changing the total mass  $\phi$  nor the behavior of each particle defined by  $St$ , we can see in Fig. 10b that each particle produces a smaller individual effect on the fluid. On the other hand, the collective



(a)  $St = 0.5$



(b)  $St = 2.2$

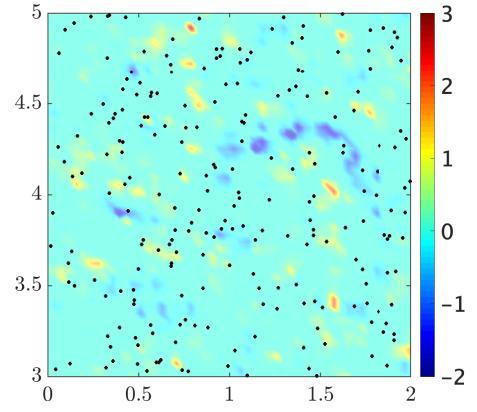
**Figure 9:** Spectral fluid-particle interaction plotted for different particle number densities and  $\phi = 0.6$ .

effect of segregated particles results in a smoother and more homogeneous two-way interaction field.

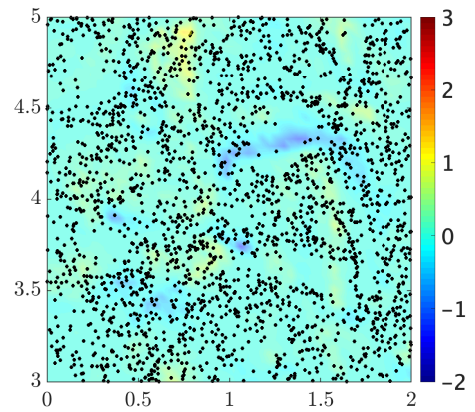
A scheme is proposed in Fig. 11 to understand how heavy isolated particles can locally produce a strong two-way interaction term whereas a more homogeneous phase will enhance global vorticity by uniformly loading the gas and therefore particles will cause the fluid to behave like a "dusty gas". Thus, distribution of a given global mass loading into different number of particles generates either localized spots or almost continuous clusters.

### 2.2.3 Radius of influence of particle

The scales of change between these two different regimes (enhancement by a heterogeneous phase at small scales and by a homogeneous one at large scales) can be measured through the wavenumbers of crossing spectra  $\kappa_{cross}$ . Figure 9a shows that this crossover of spectra takes place for  $\kappa_{cross} \in [24; 30]$ . Such wavenumbers correspond to length scales of size 0.15 to 0.3. Temporal evolution of the crossing wavelength is plotted in Fig. 12 for different particle parameters. This crossing wavelength seems weakly

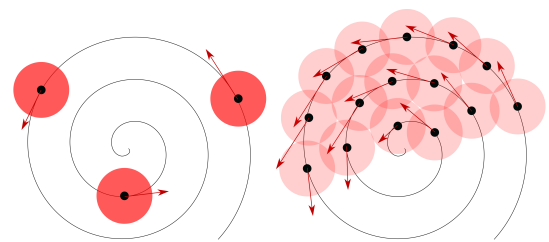


(a)  $\tilde{\psi}_p$  field for low particle number density  $n_\eta = 0.02$ . Two-way interaction energy rate is given by  $\langle \tilde{\psi}_p \rangle = \psi_p = 0.040$



(b)  $\tilde{\psi}_p$  field for high particle number density  $n_\eta = 0.2$ . Two-way interaction energy rate is given by  $\langle \tilde{\psi}_p \rangle = \psi_p = 0.037$

**Figure 10:** Distribution of two-way interaction energy rate  $\tilde{\psi}_p$  at  $t = 4.6$  superimposed with particles parametrized by  $\phi = 0.3$  and  $St = 0.25$ .



(a) Heavy isolated particles (b) Group of light particles

**Figure 11:** Schematic representation of the particles (in black) and their radius of influence (in red shades) on the fluid. Isolated particles (a) and group of particles (b).

dependent on the Stokes number. Figure 12 suggests that the scales for which isolated particles produce stronger coupling than a homogeneous disperse phase enlarge with time and with mass loading.

In Fig. 13, we propose a measure of the disturbance of the flow by a particle, by comparing flow velocities at distance  $r$  of the inertial particle with and without the reverse coupling force:  $\langle |\frac{\mathbf{u}_{f,1-way} - \mathbf{u}_{f,2-way}}{\mathbf{u}_{f,1-way}}(\mathbf{x}_p(t) + r)| \rangle$ . The log-log

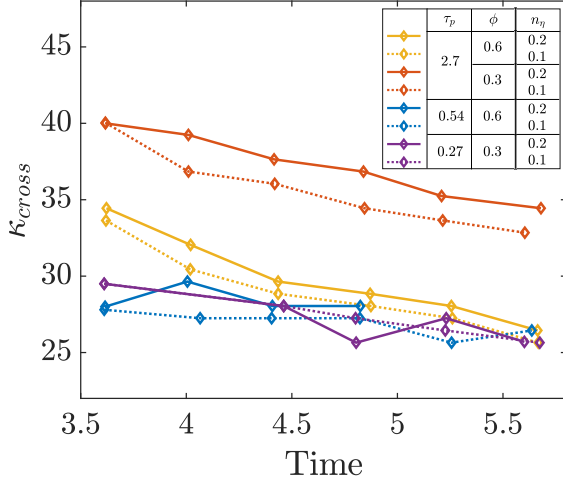


**Figure 12:** Temporal evolution of wavelength of crossing spectra (between homogeneous and lower particle number densities). Different  $St$  and  $\phi$  were tested.

scale plot of the disturbance retrieves a slope of -3, characteristic of the Stokeslet. Indeed, Saffman (1973) showed that the fluid velocity disturbance due to the presence of a particle decays as the sum of two contributions, a long-range one as  $1/r$  and a short-range one (more important for particles with  $d_p < \eta$ ) as  $1/r^3$ .

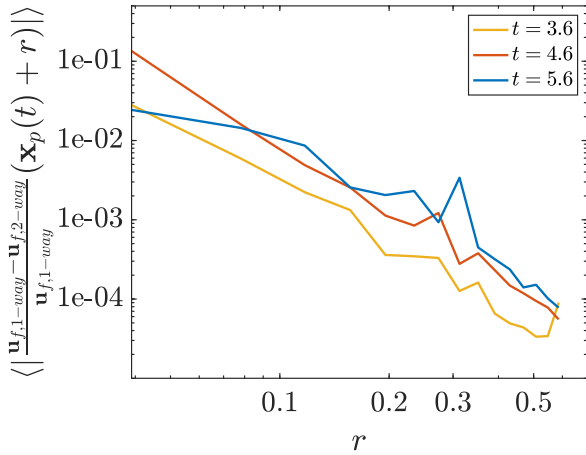
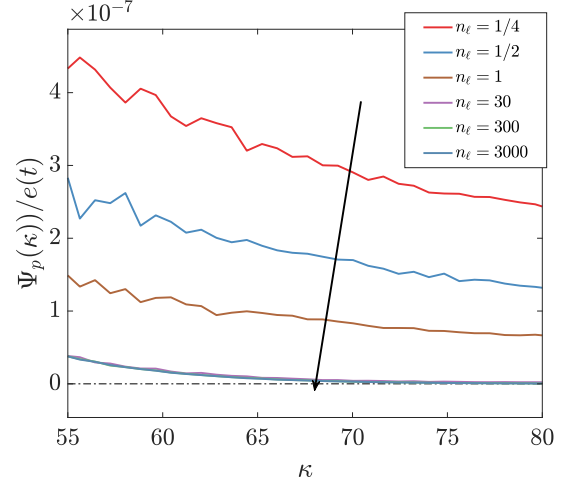
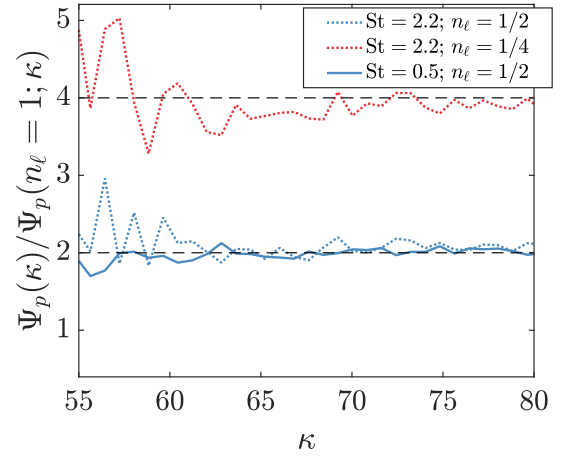


**Figure 13:** Mean temporal evolution of the fluid perturbation at distance  $r$  around inertial isolated particles.

We can also point out that the radius of the disturbance (hereinafter referred to as the radius of influence of particles) increases over time, along with the decrease of  $\kappa_{cross}$ , or the increase of some characteristic fluid scales. Thus, for a point-particle model such as the one used here, we can assume that the radius of influence of the particles will be bounded by (or at least related to) the integral length scale. Indeed, the integral length scale  $\ell$  measures the correlation distance of a process in the turbulence. It looks at the overall memory of the process and how it is influenced by previous positions and parameters. Therefore, given our results and the characterization of  $\ell$ , we assume that the radius of influence of particles should be limited by the integral length scale and we introduce the particle number density per integral length scale noted  $n_\ell = n_0 \ell^3$ .



**(a)**  $\Psi_p$  spectra for  $\phi = 0.001$  and  $St = 0.5$ .  $n_\ell$  decreases with the arrow.



**(b)** Ratio of fluid-particle spectra with  $n_\ell < 1$

**Figure 14:** Modulation of the spectral two-way interaction term at small scales. Under the threshold  $n_\ell < 1$ , a proportionality to particle individual mass is retrieved.

To study very heterogeneous disperse phase at fixed mass loading, we ran simulations with  $\phi = 0.001$  such that all our modeling assumptions (particle-point modeling, dilute regime...) remain true for the parameters of the disperse phase. Figure 14a compares the fluid-particle interaction spectra for different particle number densities  $n_\ell$ . Below the limit of one particle in the radius of influence, the fluid-particle exchange term must be proportional to the mass of the isolated particle. We retrieve this proportionality on ratios of spectra in Fig. 14b since the spectral energy level for small scales at  $n_\ell = 1/2$  is twice that for  $n_\ell = 1$  and similarly for  $n_\ell = 1/4$ , it is 4 times higher. On the other hand, as soon as the radii of influence overlap (i.e.  $n_\ell > 1$ ), the combined effect of relatively close particles generates a more complex interaction with the fluid that can no longer be described by a simple proportionality.

## Conclusion

An exhaustive study of the influence of the three parameters describing a monodispersed phase on isotropic homogeneous turbulence has been carried out. Classical results from the literature have been retrieved, in particular the global trends in energy and spectral statistics with the number of

Stokes and mass loading. The study of the two-way coupling term here normalized by fluid kinetic energy and the use of a Stokes number based on instantaneous Kolmogorov scales have permitted to clearly identify two regimes: a first regime for  $St < 1$  in which particles promote turbulent energy, and a second regime for  $St > 1$  in which particles destroy turbulent energy. Additionally to the existing literature, the present study have emphasized on the influence of the particle number density on the coupling term and have identified two non-dimensional numbers of interest:

- the normalized number density with respect to Kolmogorov scale  $n_\eta$ : for  $n_\eta < 1$ , the disperse phase is in the statistically-converged limit and behaves as a continuum; for  $n_\eta > 1$ , particles start to promote energy at small scale compared to the continuum limit, and this energy promotion is clearly weighted by mass loading but seems to be independent of the number of Stokes;
- the normalized number density with respect to Kolmogorov scale  $n_\ell$ : this number delineates the transition to a regime in which the influence of each particle is clearly isolated, and for which the radii of influence of particles do not cross.

## References

- A. H. Abdelsamie and C. Lee. Decaying versus stationary turbulence in particle-laden isotropic turbulence: Turbulence modulation mechanism. *Physics of Fluids*, 2012.
- M. Boivin, O. Simonin, and K. D. Squires. Direct numerical simulation of turbulence modulation by particles in isotropic turbulence. *Journal of Fluid Mechanics*, 375:235–263, 1998.
- J. Capecelatro and O. Desjardins. An Euler-Lagrange strategy for simulating particle-laden flows. *Journal of Computational Physics*, 238:1–31, 2013.
- C. T. Crowe, M. P. Sharma, and D. E. Stock. The particle-source-in cell (PSI-CELL) model for gas-droplet flows. *Journal of fluids engineering*, 99(2):325–332, 1977.
- O. A. Druzhinin. The influence of particle inertia on the two-way coupling and modification of isotropic turbulence by microparticles. *Physics of Fluids*, 13(12):3738–3755, 2001.
- O. A. Druzhinin and S. Elghobashi. On the decay rate of isotropic turbulence laden with microparticles. *Physics of Fluids*, 11(1999):602, 1999.
- J. K. Eaton and J. R. Fessler. Preferential concentration of particles by turbulence. *International Journal of Multiphase Flow*, 20:169–209, 1994.
- S. Elghobashi and G. C. Truesdell. On the two-way interaction between homogeneous turbulence and dispersed solid particles. I: Turbulence modification. *Physics of Fluids A: Fluid Dynamics*, 5(7):1790–1801, jul 1993.
- A. Ferrante and S. Elghobashi. On the physical mechanisms of two-way coupling in particle-laden isotropic turbulence. *Physics of Fluids*, 15(2):315–329, 2003.
- P. Février, O. Simonin, and K. D. Squires. Partitioning of particle velocities in gas-solid turbulent flows into a continuous field and a spatially uncorrelated random distribution: Theoretical formalism and numerical study. *Journal of Fluid Mechanics*, 533:1–46, 2005.
- K. Fröhlich, L. Schneiders, M. Meinke, and W. Schröder. Validation of Lagrangian Two-Way Coupled Point-Particle Models in Large-Eddy Simulations. *Flow, Turbulence and Combustion*, 2018.
- G. Mallouppas, W. K. George, and B. G. M. van Wachem. New forcing scheme to sustain particle-laden homogeneous and isotropic turbulence. *Physics of Fluids*, 2013.
- G. Mallouppas, W. K. George, and B. G. van Wachem. Dissipation and inter-scale transfer in fully coupled particle and fluid motions in homogeneous isotropic forced turbulence. *International Journal of Heat and Fluid Flow*, 2017.
- M. R. Maxey, B. K. Patel, E. J. Chang, and L.-P. Wang. Simulations of dispersed turbulent multiphase flow. *Fluid Dynamics Research*, 20(1):143–156, 1997.
- C. Poelma, J. Westerweel, and G. Ooms. Particle-fluid interactions in grid-generated turbulence. *Journal of Fluid Mechanics*, 589:315–351, 2007.
- S. B. Pope. *Turbulent Flows*. Cambridge university press, 2000.
- J. Reveillon and F.-X. Demoulin. Evaporating droplets in turbulent reacting flows. *Proceedings of the Combustion Institute*, 31 II:2319–2326, 2007.
- P. G. Saffman. On the stability of laminar flow of a dusty gas. *Journal of Fluid Mechanics*, 13(1):120–128, 1962.
- P. G. Saffman. On the Settling Speed of Free and Fixed Suspensions. *Studies in Applied Mathematics*, 52(2):115–127, jun 1973.
- K. D. Squires and J. K. Eaton. Particle response and turbulence modification in isotropic turbulence. *Physics of Fluids A: Fluid Dynamics*, 2(7):1191–1203, jul 1990.
- K. D. Squires and J. K. Eaton. Effect of Selective Modification of Turbulence on Two-Equation Models for Particle-Laden Turbulent Flows. *Journal of Fluids Engineering*, 116 (December 1994):778, 1994.
- H. C. Strutt, S. W. Tullis, and M. F. Lightstone. Numerical methods for particle-laden DNS of homogeneous isotropic turbulence. *Computers and Fluids*, 2011.
- S. Sundaram and L. R. Collins. A numerical study of the modulation of isotropic turbulence by suspended particles. *Journal of Fluid Mechanics*, 379:105–143, 1999.
- A. Vié, H. Pouransari, R. Zamansky, and A. Mani. Particle-laden flows forced by the disperse phase: Comparison between Lagrangian and Eulerian simulations. *International Journal of Multiphase Flow*, 79:144–158, 2016.
- R. Zamansky, F. Coletti, M. Massot, and A. Mani. Radiation induces turbulence in particle-laden fluids. *Physics of Fluids*, 26(7):71701, 2014.